

Cantilevers with integrated sensor for time-resolved force measurement in tapping-mode atomic force microscopy

A. F. Sarioglu^{a)} and O. Solgaard

E. L. Ginzton Laboratory, Stanford University, Stanford, California 94305, USA

(Received 7 June 2008; accepted 17 June 2008; published online 16 July 2008)

We present a micromachined cantilever with an integrated high-bandwidth resonator for direct measurement of tip-sample interaction forces in tapping-mode atomic force microscopy. Force measurements are achieved by a diffraction grating that serves as a differential displacement sensor for the tip motion relative to the cantilever body. Time-resolved tip-sample interaction force measurement is demonstrated on a silicon sample following calibration of the probe structure. By using lock-in detection, the harmonics of periodic tip-sample interaction have been utilized to obtain high-contrast, material specific images. The harmonic images of patterned silicon/silicon nitride control samples and triblock copolymers are presented. © 2008 American Institute of Physics.

[DOI: 10.1063/1.2959828]

Atomic force microscope¹ (AFM) is widely used for nanoscale surface characterization. There is an increasing interest in its use for mapping of material specific surface properties. Quasistatic methods, such as nanoindentation,² and several dynamic methods, such as ultrasonic force microscopy,³ pulsed-force microscopy,⁴ and force modulation microscopy,⁵ have been developed for local stiffness measurements. These techniques generally suffer from low operational speeds and require large forces applied to the surface under test, limiting their use on soft materials such as biological samples.

Tapping-mode AFM⁶ is the preferred operational mode, especially on soft samples. In tapping-mode, phase information⁷ and higher harmonic signals⁸ can be used to obtain nanoscale maps of material characteristics. Measurement of tip-sample interaction forces is a more direct method for material characterization. Recently, measurements of tip-sample interaction have been demonstrated by specially designed probes.^{9,10}

In this paper, we report a method for time-resolved measurement of tip-sample interaction forces by using a micromachined cantilever with an integrated high-bandwidth force sensor. A small and stiff mechanical resonator on the cantilever provides the necessary temporal resolution for observing tip-sample interactions. The cantilever itself serves two purposes. First, being softer, it limits the amount of repulsive force applied to the surface. Secondly, it provides the necessary oscillation amplitude for the smaller sensor to interact with the surface in a tapping-mode configuration. A scanning electron microscope (SEM) image of the micromachined probe is given in Fig. 1. The small resonator on the cantilever forms a phase sensitive diffraction grating that serves as a relative displacement sensor for tip motion. This type of grating has earlier been used to measure the displacement of cantilevers in contact mode AFM.¹¹

In operation, the cantilever is driven close to its fundamental resonance frequency. During a small fraction of the oscillation cycle, the tip interacts with the sample. The high-bandwidth force sensor responds to the interaction force, whereas the larger and softer cantilever cannot follow effi-

ciently because of its lower bandwidth. That causes the relative position of the diffractive grating fingers to change, modifying the amount of light in the diffracted modes. By measuring the light intensity variation in the diffracted modes, the tip-sample interactions are observed.

Our cantilever has the advantage of achieving high temporal resolution by reducing the displaced mass rather than purely increasing the stiffness, which would cause lower signal-to-noise ratio (SNR). In addition, the use of interdigitated fingers provides completely differential interferometric measurement, minimizing crosstalk between cantilever oscillations and tip motion.

The design of cantilevers with force sensors requires several specific considerations. First of all, the interdigitated fingers of the differential sensor should be fabricated such that the adjacent fingers have $\lambda/8$ offset, where λ is the illumination wavelength. This provides maximum sensitivity and linearity for measuring weak tip-sample interaction that causes small relative displacements on the order of 1 nm or

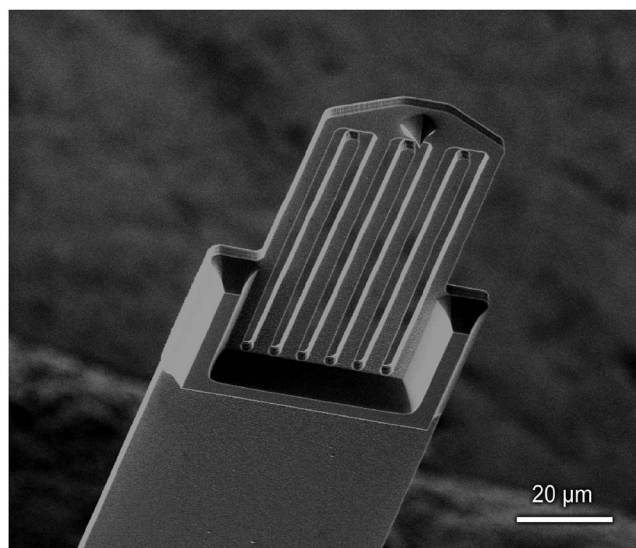


FIG. 1. SEM micrograph of a cantilever with integrated force sensor. The cantilever is 370 μm long, 60 μm wide, and 2.5 μm thick. The grating fingers of the interferometric force sensor are 3 μm wide and 70 μm long.

^{a)}Electronic mail: sarioglu@stanford.edu.

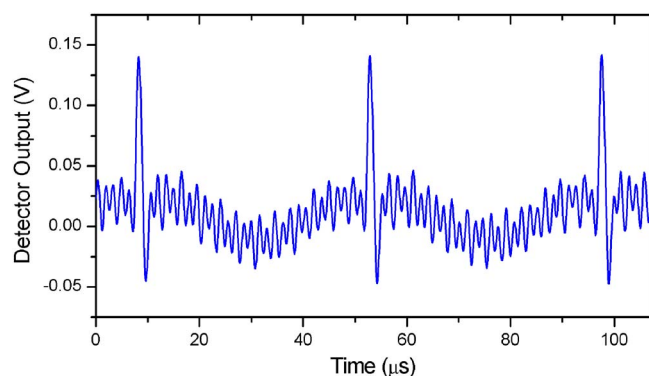


FIG. 2. (Color online) Oscilloscope traces of individual tapping events on a Si sample.

less. Secondly, the coupling between flexural resonances of the cantilever and the force sensor should be minimized so that the force sensor can be modeled as a simple harmonic oscillator. This is achieved by designing the reference fingers and fingers connected to the tip to have equal resonance frequencies. The fingers connected to the tip have additional mass, so their resonance frequency will be lower if no balancing is performed. The resonance frequencies of adjacent fingers are equalized by designing the outer fingers to be shorter by incorporating thick support regions around the fingers.

The cantilevers are fabricated with standard optical lithography in a four-mask process that requires wafer bonding. The process starts with silicon on insulator (SOI) wafers with 10 μm device layers. First, the offset between grating fingers is defined using local oxidation of silicon. A 40 nm thick SiO_2 layer is grown, followed by an 80 nm Si_3N_4 deposition. The nitride layer is patterned and followed by an oxidation process that removes silicon from areas that are not covered with silicon nitride without affecting the surface roughness. After removal of nitride and oxide layers, another silicon wafer with thermal oxide is fusion bonded to the SOI device layer. The substrate of the SOI wafer is removed using tetramethylammonium hydroxide. The tips and the support regions are patterned in the oxide layer using 6:1 buffered oxide etch (BOE) and formed by undercutting SF_6 plasma etching. The tips are oxide sharpened at 950 $^\circ\text{C}$. The cantilever outline with sensor gratings is patterned in a plasma etch. The top surface is covered with tetraethyl orthosilicate and silicon nitride. The handle wafer is etched using KOH through a nitride mask from the backside. Finally, the structures are released in a nitride plasma etch followed by a 6:1 BOE etch.

We performed time-resolved interaction force measurements with a commercial AFM¹² combined with a custom photodetector circuit. The cantilever was excited close to its fundamental resonance frequency at 22 kHz. The resonance frequency of the force sensor was measured to be 672 kHz. A 690 nm laser light was focused to a $30 \times 30 \mu\text{m}^2$ spot on the integrated diffraction grating force sensor on the cantilever. The zeroth and first modes of the diffraction pattern were placed on each half of an external dual-cell photodiode. The individual cell outputs were subtracted from each other and low-pass filtered with a 1 MHz bandwidth. The measured signal is presented in Fig. 2. The ringing that is apparent in the trace is due to the resonance of the small force sensor and coupling of the force sensor to cantilever resonances. The

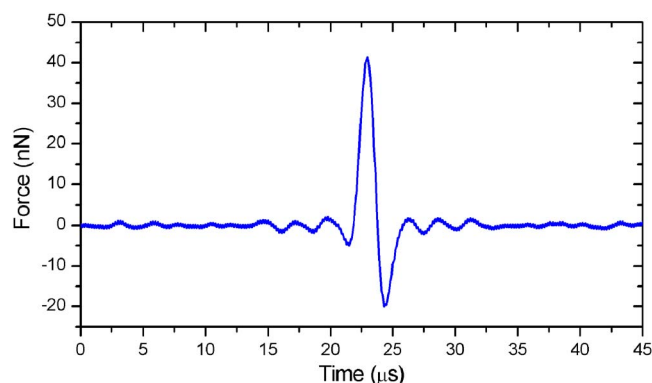


FIG. 3. (Color online) Time-resolved tip-sample interaction force curve obtained on a Si sample. The maximum attractive forces on approach and during retraction are 4.93 nN and 19.97 nN, respectively. The maximum repulsive force is 41.26 nN. The tip-sample interaction corresponds to 6% of the cantilever oscillation period.

effect of sensor resonance can be compensated by inverse filtering the displacement signal.^{10,13,14} In our experiments, the transfer function of the force sensor is modeled as a damped, simple harmonic oscillator. The resonance frequency and the quality factor of the sensor are determined experimentally by sweeping the cantilever driving frequency. This lets us observe the sensor resonance, because a small mismatch between the resonance frequencies of the stationary and moving grating fingers causes relative displacement when the cantilever is driven close to the sensor resonance frequency. The accuracy of the calibration parameters is confirmed by observing tip-sample rupture events. In addition to inverse filtering, nonlinear least square fitting was performed on the signal for the time periods in which the tip is not in contact with the sample. During this process, the harmonics of the driving signal were used as the basis set. Together with inverse filtering, this lets us remove the errors caused by misplacement of the photodiode, photodetector nonlinearity, and coupling between flexural resonances of the cantilever and the force sensor.

The force constant of the cantilever is estimated by finite element analysis to be 0.74 N/m. The force calibration of the integrated force sensor is performed by pressing the cantilever on a hard surface. The total force acting on the tip is calculated by multiplying the piezotube displacement with the estimated spring constant of the cantilever. The resulting change in the photodiode signal is measured. The time-resolved force signal following calibration and signal processing is given in Fig. 3. The attractive, repulsive, and adhesive phases of the tip-sample interaction can be identified with μs time resolution. The hysteresis in tip-sample interaction is also apparent from the measurements.

Our cantilever can be used in commercial AFMs in two ways. One is to align one of the diffracted modes to the center of the quadrant photodiode and block the others. In this setting, the vertical displacement of the spot corresponds to cantilever oscillations and the total power on the quadrant photodiode corresponds to relative tip displacement due to interaction with the sample. The other scheme is to align two adjacent diffracted modes onto the left and right halves of the quadrant photodiode such that they are vertically centered. In this setting, the vertical difference signal corresponds to cantilever oscillations and the lateral difference signal gives the tip displacement relative to the cantilever body. We chose the

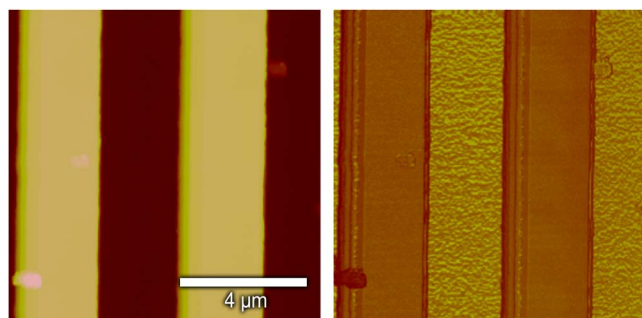


FIG. 4. (Color online) Topography (left) and simultaneously acquired 28th harmonic image (right) of Si_3N_4 stripes on a Si substrate imaged with our probe. (Scan size: $10 \times 10 \mu\text{m}^2$.)

second method for the images reported in this paper. In this setting, differential measurement minimizes common mode noise due to laser diode intensity and wavelength instabilities and two spatially separated diffraction modes on the photodiode eliminate crosstalk between vertical and lateral signals in tapping-mode operation.

In tapping-mode AFM, the tip-sample interaction is quasiperiodic and the frequency spectrum consists of harmonics of the cantilever excitation frequency. The tip-sample interaction depends on material parameters, so the amount of signal power at each harmonic is a function of sample properties.¹⁵ This provides a contrast mechanism for obtaining material specific AFM images.

We performed imaging on a Si sample with $3 \mu\text{m}$ wide, 670 nm high low-stress Si_3N_4 lines with our cantilevers in a commercial AFM.¹² By use of a lock-in amplifier, the signal power at the 28th harmonic is recorded as the harmonic image data signal. The topography image and the 28th harmonic image are shown in Fig. 4. The harmonic image shows contrast between Si and Si_3N_4 surfaces and the material boundaries are very clearly observed. Moreover, the harmonic image clearly shows the roughness of the Si surfaces, caused by reactive ion etching of Si_3N_4 .

We also used our probes on thin films of polystyrene-block-polybutadiene-block-polystyrene (SBS) triblock copolymer in a commercial AFM.¹⁶ At room temperature, the polybutadiene blocks are above their glass transition temperature, whereas the polystyrene blocks are in glassy state. This results in local stiffness variations on length scales around 50 nm .¹⁷ Figure 5 shows the topography and 17th harmonic image of the sample. The microphase separation is revealed by the harmonic image. The bright and dark regions in the 17th harmonic image correspond to stiff polystyrene blocks and compliant polybutadiene blocks respectively.

In summary, we have designed and fabricated cantilevers that have integrated force sensors for observing tip motion

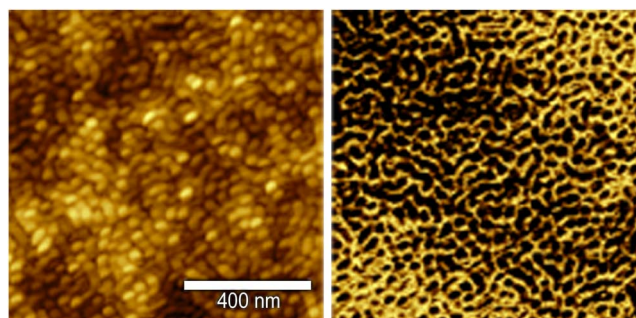


FIG. 5. (Color online) Topography (left) and simultaneously acquired 17th harmonic image (right) of thin film of SBS triblock copolymer imaged with our probe. (Scan size: $1 \times 1 \mu\text{m}^2$.)

relative to the cantilever body. This let us observe tip-sample interactions with high SNR. We demonstrated time-resolved measurement of tip-sample interaction forces in tapping-mode AFM, and we used our probes to obtain harmonic images of samples containing materials with different mechanical properties.

The authors would like to thank Maozi Liu of Agilent Technologies for the polymer sample. This work was supported by NSF PHY-0425897, DARPA under Grant No. HR0011-06-1-0049, and Boeing under Contract No. SPO #33130.

¹G. Binnig, C. F. Quate, and C. H. Gerber, *Phys. Rev. Lett.* **56**, 930 (1986).

²N. A. Burnham and R. J. Colton, *J. Vac. Sci. Technol. A* **7**, 2906 (1989).

³K. Yamanaka, H. Ogiso, and O. Kolosov, *Appl. Phys. Lett.* **64**, 178 (1994).

⁴H. Krottil, T. Stifter, H. Waschipyk, K. Weishaupt, S. Hild, and O. Marti, *Surf. Interface Anal.* **27**, 336 (1999).

⁵P. Maivald, H. J. Butt, S. A. C. Gould, C. B. Prater, B. Drake, J. A. Gurley, V. B. Elings, and P. K. Hansma, *Nanotechnology* **2**, 103 (1991).

⁶Q. Zhong, D. Innis, K. Kjoller, and V. B. Elings, *Surf. Sci. Lett.* **290**, L688 (1993).

⁷J. Tamayo and R. Garcia, *Appl. Phys. Lett.* **71**, 2394 (1997).

⁸R. W. Stark and W. M. Heckl, *Rev. Sci. Instrum.* **74**, 5111 (2003).

⁹A. G. Onaran, M. Balantekin, W. Lee, W. L. Hughes, B. A. Buchine, R. O. Guldiken, Z. Parlak, C. F. Quate, and F. L. Degertekin, *Rev. Sci. Instrum.* **77**, 023501 (2006).

¹⁰O. Sahin, S. Magonov, C. Su, C. F. Quate, and O. Solgaard, *Nat. Nanotechnol.* **2**, 507 (2007).

¹¹S. R. Manalis, S. C. Minne, A. Atalar, and C. F. Quate, *Appl. Phys. Lett.* **69**, 3944 (1996).

¹²DIMENSION 3100, Nanoscope IIIa, Veeco, Santa Barbara, CA.

¹³M. Stark, R. W. Stark, W. M. Heckl, and R. Guckenberger, *Proc. Natl. Acad. Sci. U.S.A.* **99**, 8473 (2002).

¹⁴J. Legleiter, M. Park, B. Cusick, and T. Kowalewski, *Proc. Natl. Acad. Sci. U.S.A.* **103**, 4813 (2006).

¹⁵O. Sahin, A. Atalar, C. F. Quate, and O. Solgaard, *Phys. Rev. B* **69**, 165416 (2004).

¹⁶Agilent 5500 AFM, Agilent Technologies, Chandler, AZ.

¹⁷S. N. Magonov, J. Cleveland, V. Elings, D. Denley, and M.-H. Whangbo, *Surf. Sci.* **389**, 201 (1997).